Deep Choroid Layer Extraction from OCT Images

Saleha Masood
Shanghai Jiao Tong University
Shanghai 200240, China
Salehamasood08@gmail.com

Sheng Bin
Shanghai Jiao Tong University
Shanghai 200240, China
shengbin@cs.sjtu.edu.cn

Zhenyu Song
Shanghai Jiao Tong University
Shanghai 200240, China
sunnyszy@sjtu.edu.cn

Abstract

Choroid layer is a layer of tissues located at the back end of the retina and OCT technology is mainly used to image this retinal feature. Various studies have proven that the thickness of choroidal is correlated with the diagnosis of several ophthalmic diseases. Despite the contemporary advances, automatic segmentation of choroid layer is still a challenging task because of the low contrast of OCT images. Majority of the existing methodologies carries out segmentation manually or by following semi-automatic approaches. In this paper, we proposed a novel and effective approach which qualitatively improves the automatic segmentation of the choroid layer. Rather than using Convolutional Neural Network (CNN) as a classifier, proposed method used it as a feature generator to extract useful features form the image. Together with CNN features, some textural features were also extracted from the image. The textural features being extracted include Gabor features, haar features and gray level co-occurrence features. The proposed method was regularized by combining CNN feature vector with the textural or handcrafted features. For the classification purpose, a separate Support Vector machine was trained using each of the feature type. All the trained SVM's were than linearly combined for the final segmentation of choroid layer. The Proposed method was tested on a database of 525 images of real patients from Hospital No.6 of Shanghai. In addition, we proposed two quantitative metrics for the error calculation of the pixel wise error in the segmentation and an average error in the thickness map being generated. The experimental results proved that the proposed method out performs previous segmentation approaches by achieving an accuracy of 97% with a mean error rate of 2.84.

1. Introduction

Measuring the thickness of the human choroid through the use of OCT (optical coherence tomography) images is of great significance for clinical and academic use. It gives insight into the anatomy and physiology of the eye in addition to the information regarding refractive error and eye diseases [1].The vascular layer of the eye lies between retina and sclera and is termed as choroid or choroid coat. Its function is to give metabolic support to RPE (retinal pigment epithelium) and also to supply blood to optic nerve. Anatomically, the choroid can be divided into two principal components: the choriocapillaris, a lobular, vascular plexus comprised of large fenestrated capillaries adjacent to Bruch's membrane, and the choroidal stroma. Changes in the health of the choroid have been documented in early macular degeneration and in advanced diseases. Quantitative and qualitative analysis of bruch's membrane and choroid layer can help to analyze the relationship between the various retinal diseases.

Optical coherence tomography (OCT) is a latest technology to examine the internal structure of retina. It is an acute imaging technology that helps to take cross section of retinal layers with the use of light waves. Decrease in the topographic data's wealth of a feature by rim area or by other retinal lesions results in waste of the useful information. Statistical shape examination has a potential to provide useful information in an automated way that can help in the diagnosis of various diseases effectively. Clinical assessment process is highly dependent on the segmentation methods of retinal images using OCT technology. Various image processing techniques have been proposed and implemented in order to mend the clinical advantage of OCT technology.

Segmentation of choroid layer illustrates methods based on machine learning, tracking based and intensity based approaches. Each method focuses on different type of features for the segmentation purpose. Main categories of segmentation methods focus on retinal layering structures or fluid filled areas to make clinical decisions regarding disease identification.

Analysis of the existing approaches shows that the optimal accuracy was achieved using machine learning approaches. Traditional methods in the prospect of retinal image segmentation are based on intensity based image information or statistics provided by image gradient. These intensity based methods fails to segment out the region of interest accurately because of the low contrast and poor quality of OCT images. Tracking based approaches requires some seed points in advance and are interactive whereas intensity based approaches cannot provide promising results. Deep learning methods have a potential to overcome the existing challenges and to improve the segmentation accuracy.

There are certain challenges in the accurate segmentation of the choroid layer. Most of the segmentation methods perform manual segmentation. Image analysis is subjective in nature which requires the trainer to be trained perfectly. These manual measurement are time taking and very arduous with unclear and ambiguous repeatability. Major challenges in accurate segmentation of the choroid layer are as follows:

- The histogram of choroid layer and sclera is inseparable because the OCT images are of very low contrast.
- The choroid layer has inconsistent texture and inhomogeneous intensity.
- The sclera and choroid layer has a week interface.

With progress in segmentation methods certain complex image processing approaches were also used for retinal layer segmentation. These methods include graph cut, active contour and active shape models, support vector machines etc. So starting with a texture features analysis, [5] retinal layers were segmented by the combination of diffusion filtering and structure tensor. The approach also makes use of B-Scans. Active contour model has also been used for the segmentation of retinal layers [6]. Later active contour model was used in combination with kernel based optimization for the layers segmentation [7]. The use of information extracted from image gradient and intensity statistics was later used for the choroid layer segmentation [8]. Certain other image processing techniques used for segmentation purpose include markov random field [9] and support vector machine [10]. The shape and texture of image features was also analyzed in this context [11]. Various graph search based image processing approaches have also been used for the segmentation of retinal layering structure. The combination of dynamic programing and graph search approach is carried out in [12][13]. The same approach was then further extended to segment out the anterior features of retina [14]. Concept of dual scale gradient statistics with the graph cut approach for retinal layers segmentation is carried out in [15]. Texture based statistics utilization was also implemented to segment out retinal layers [16]. Graph cut method with the combination of volumetric data for segmentation can be analyzed in [17]. Hard-soft constraints for segmentation are presented in [18]. 3D graph search algorithm is also proposed and implemented in the prospect of retinal layers [19]. Automatic segmentation of choroidal boundary in OCT images using a statistical model has been recently described in [20]. Another automatic choroidal vessel segmentation approach is carried out in [21], however the method mainly focus on vascular structure instead of choroidal thickness. Another semi-automatic choroid layer segmentation approach based on graph search has been presented in [22]. A fully automatic graph cut method with the combination of pixel valley for choroid layer segmentation was proposed and implemented by Tian et al [23]. Three dimensional graph cut method for automatic retinal layers segmentation have been reported in [24] [25].

The focus of this research is to overcome the existing challenges in the context of choroid layer segmentation and to provide an automatic segmentation approach. After segmenting choroid layer, thickness of choroid layer was measured so that this qualitative analysis of choroid layer can help to diagnose different retinal based disease. To achieve these goal different types of features were extracted from the image. The main purpose of using different types of features was to extract as much useful information as possible from the image to increase the segmentation accuracy and to decrease the error rate. The proposed approach used two methodologies to segment out sclera and choroid layer. In order to segment out choroid layer two boundaries need to be segmented. The required boundaries include Bruch's Membrane (BM) and choroid layer. As the OCT images are of low contrast, and choroid layer have a tabular and narrow band like structure, it is difficult to segment out this boundary. On the other hand, segmentation of inner boundary called Bruch's Membrane is relatively easy. So in the proposed method, BM was segmented out using a series of morphological operations where as in order to segment out choroid layer, more detailed image statistics were required. In order to segment out choroid layer various textural features together with CNN feature vector were extracted from the image. And SVM was used for the classification purpose.

The main contributions of the research include:

- We proposed a two stage automatic choroid layer segmentation approach which concurrently considers the segmentation accuracy and consistency of the method.
- A novel segmentation model, which combines deep learning features with some handcrafted features to get more intrinsic and high level features.
- CNN was used as a feature generator rather than a classifier.
- The proposed method was tested on the data of real patients. Experimental results showed that the proposed method provided high accuracy rate and minimized the error rate to a great extent.

The remainder of the paper is organized as follows: Section II is devoted to the details of the proposed methodology. Experimental results with the quantitative analysis of the proposed method are presented in section III. Finally the conclusion and future directions are discussed in the last section.

2. Materials and Methods

The methodology being adapted in this research is based on the combination of deep learning and hybrid features approach. The proposed method works for the

accurate segmentation of the choroid and sclera layer. The hybrid approach is based on the theories of convolutional neural networks and some handcrafted features including gabor features, gray level co-occurrence matrix and haar features. Quantification of chroidal thickness depends on the segmentation of two layers. The required layers include Bruch's membrane and the choroidal-scleral interface. So the proposed approaches can be divided into two phases. One is the segmentation of Bruch's membrane followed by the segmentation of choroidal-scleral interface. Fig 1 depicts the required retinal boundaries.

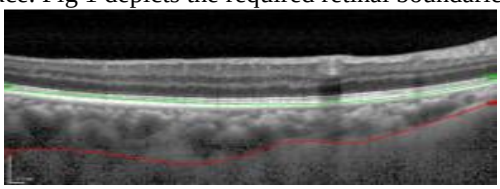

Fig 1 OCT image with segmented Bruch's Membrane and Choroid layer. The upper green line represents the Bruch's Membrane whereas lower red line represents choroid layer. These are the two require layers to be segmented in this research.

2.1 Bruch's Membrane Segmentation:

The segmentation of Bruch's Membrane is carried out by a series of steps based on the morphological operations. The steps involved in this process are as follows:

2.1.1 Binary Conversion:

The first step carried out for the bruch's membrane is to convert the input image to binary with the help of thresholding. The optimal threshold used for the OCT images in our approach is 190. Thresholding was mainly applied to extract those pixels from the image which corresponds to an object in the image. The acquired information from thresholding process results in binarized data with a range of different intensities. The pixels with same intensity value are considered as the foreground pixels whereas rests of the pixels are set to background.

$$\boldsymbol{bin - \varphi_{k1}(f)(x) = 1 \quad if\ f(x) \geq k1}$$
$$\boldsymbol{bin - \varphi_{k1}(f)(x) = 0 \quad otherwise} \quad (1)$$

Where f is the gray scale input image and φ_{k1} is the representing threshold value by a non-negative integer *k1* and bin is the resulting binary image. The default value is 1. The optimal threshold used for OCT images was set to 190.

2.1.2 Opening operation:

After we acquired the binary image, next an opening operation is applied in order to remove the noise form the image. The opening operation is basically a combination of two operations i.e. erosion followed by a dilation process. The basic purpose to apply opening operation was to remove dark pixels (i.e. noise) from the foreground pixels of the object and to figure out certain required shapes from the image.

$$\boldsymbol{f \circ s = (f \ominus s) \oplus s} \quad (2)$$

where f is the input image and s is the structuring element (SE).

2.1.3 Selection Operation:

Next the numbers of rows spanned by the extracted object were considered. For selection of such rows certain range was defined. The range was selected which contained most of the points. The points outside the defined range were eliminated.

2.1.4 Thinning Operation:

The morphological thinning operation was then applied in order to remove certain foreground pixels which are not part of the region of interest. The thinning operation of an image f by a structuring element s can be expressed as follows:

$$\boldsymbol{Thin\ (f, s) = f - hit\ and\ miss\ (f, s)} \quad (3)$$

If the background and foreground pixels of the input image exactly match the foreground and background pixel of the structuring element then it was considered as object part otherwise it as set to background pixel.

2.1.5 Polynomial Fitting:

The last step to draw the Bruch's Membrane layer was to apply polynomial fitting.

In order to apply the polynomial the general form of order j is considered:

$$\boldsymbol{f(x) = a_0 + a_1 x + a_2 x^2 + a_3 x^3 + \cdots + a_j x^j = a_0 + \sum_{k=1}^{j} a_k x^k} \quad (4)$$

The optimal points or coefficients that best fits the line curve were selected based on the minimum error criteria. The coefficients which gave the minimum error among the data y and optimally fitted f(x) were taken as the regions to be fitted in the curve. The error calculation was carried out by the following expression:

$$\boldsymbol{err = \sum_{i=1}^{n} [y_i - [\, a_0 + \sum_{k=1}^{j} a_k x^k]]^2} \quad (5)$$

Where j is the order of polynomial, n is number of the given points and i represent the summed data points. The output of this step is the final segmentation of the Bruch's Membrane layer. Fig 2 shows the result of each carried step for the segmentation of the bruch's membrane.

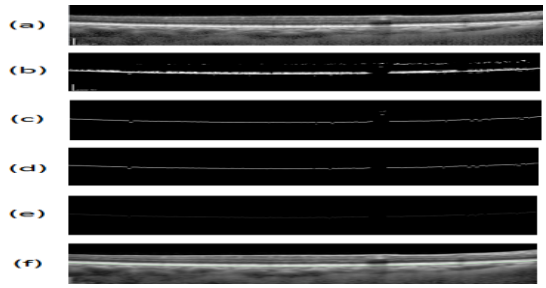

Fig 2 Bruch's Membrane segmentation steps: In the diagram given above (a) represents the input image, (b) corresponds to the result of converting input image to binary format, (c) is the result of applying opening operation, (d) represents the result of selection, (e) shows the result of thinning operation, (f) step finally apply erosion and then polynomial fitting is applied to draw the final segmented bruch's membrane area.

2.2 Choroid Layer Segmentation using Hybrid approach:

Considering the field of medical imaging it can be figured out that the data sets are not very big support in training Neural Network (NN). So medical scenerios can not be dealt well using the deep learning algorithems. However image features can be extracted effectively if the neural network is trained using a large data set. As prior knowlede of ststistics helps to get features more accuratley. The proposed method here uses a pre-trained network to extract the image features which are further used for the classification of choroid layer. Besides CNN feature vector, we generated some handcrafted features. Each group of features is used to train a support vector machine classifier. The labels produced by each test sample using the individual SVMs are then linearly combined `to obtain a label.

For the choroid layer segmentation using hybrid approach image features are extracted by four different ways. Instead of using convolutional neural network as a classifier the proposed method used it as a feature generator. The features from the image are extracted using four different approaches i.e. by using convolutional neural networks, haar wavelet transfor, gabor features and gray level co-occurrence matrix. The classification is carried out using the support vector machine. Feature vectors are extracted from each of the feature type and a separate SVM is trained using each feature. All the trained SVM are then linearly combined into a single SVM for the final classification of the choroid layer. The features work flow can be analyzed in the Fig 3 given below:

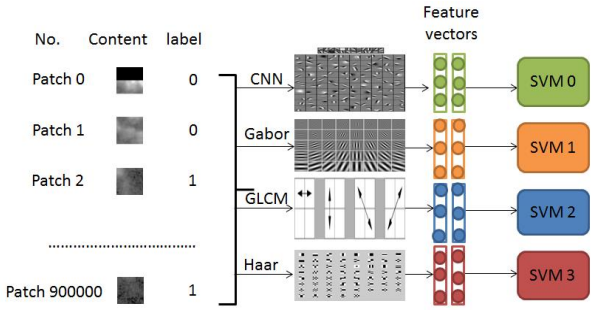

Fig 3 Hybrid Method workflow

2.2.1 CNN as a Feature Generator:

Instead of using Convolutional Neural Network (CNN) as a classifier, the proposed method used it as a feature generator. The generated features were then used for the classification purpose using Support Vector Machine (SVM). In order to extract the features from CNN, it was required to train the network using the manually segmented images.

The basic purpose of using CNN for classification was that it involves small preprocessing, which helps to train the network in a reasonable time and manner. Another main reason was little dependence of CNN on prior knowledge.

The framework used for the implementation of CNN model in our research is caffe, which is a deep learning framework. We used a pre-trained model called CIFAR-10 to generate features. CIFAR-10 is composed of a layering structure including layer of convolution, pooling followed by linear unit nonlinearities and have a linear classifier for the contrast normalization on the top of all these layers. The modification was carried out in the last layer of the CIFAR-10 model. The architecture of CNN used in our approach is shown in Fig 4:

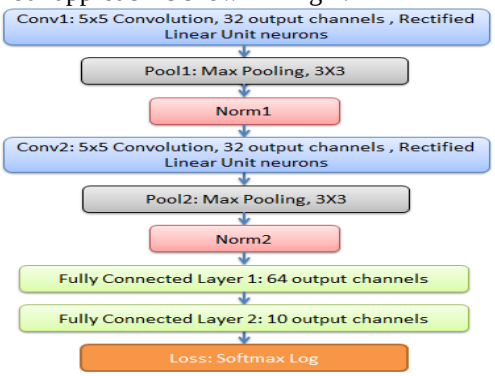

Fig 4 The CNN architecture

The description of the layers is as follows:

1. Conv1 and Conv2 layers basically represents convolutional layers with Rectified Linear Activation (RLA)
2. Pool1 and pool2 represents the max pooling layers of CNN.
3. Norm1 and Norm2 are used for local response normalization.
4. FC1 and FC2 correspond to fully connected layers with RLA.
5. SL is used for linear transformation

In order to extract features from the convolution neural network, the first required step was to train the CNN with the manually segmented images. The training process was carried out using the concept of patch training. The model was trained using the patches.

Implementation Methodology:

The first step was to collect data. The data used for experiments in our research was basically collected from the Shanghai Hospital No 6. The data of 21 individuals was provided by the doctors. Each person had 25 images representing different depth of the choroid layer. Data provided by the doctors contained human labeled images, where Bruch's Membrane and choroid layer was segmented manually in each of the image by the doctor. In order to train the CNN concept of patching was used. Here the human labeled image was analyzed patched wise. In order to sample a patch every patch of the image was analyzed in order to classify the patch on the line or off the line. Any patch contacting pixel on the lower line was

labeled as 1 and was considered on the line pixel whereas a patch contacting no pixel on the lower line was considered as off the line patch and was labeled as 0. The sampling procedure being carried can be examined in the Fig 5:

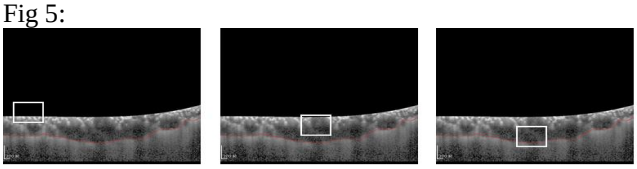

Fig 5 Patch Sampling Process: Part (a) and (b) represents examples of the case where patch contains all black pixels i.e. the patches which are not containing any pixel on line so the label in these cases will be assigned '0' value, part (c) corresponds to an example where patch contains pixel on line so here the label will be assigned a value 1

The first step carried out here was to preprocess the image. The preprocessing step mainly black out all the region above the segmented Bruch's Membrane layer so that the area to be processed can be reduced for the choroid layer segmentation. As the region above Bruch's Membrane cannot contain any part of the choroid layer, so the above region was eliminated to reduce the area to be processed for further segmentation process. After the preprocessing, next step was to sample the patches from the images. The patch size used in our research is 32x32. The patches were sampled from left to right and from top to bottom. The stride between each patch was taken as 5 pixels. A threshold was then set to discard the pixels containing too many black pixels. If a patch contains more than 1/3 black pixels, it was discarded. The dataset contains images of 21 persons. Data of 12 individuals was used to train the model whereas data of 9 individuals was used to test the model In order to balance the label 0 and 1, the patches of label 0 were randomly chosen to have the same number as label 1. There are about 3000 patches for one figure, so the total sampled patches were about 900000. Next we convert the data to binary format. The binary format for CIFAR-10 is shown in equation 6. In other words, the first byte is the label of the first image, which is a number 0 or 1. Total of 3000 patches were extracted from an image. Where first 1024 bytes represents values of red channels, next 1024 bytes are for green channel and last 1024 bytes corresponds to the blue channel values of the image.

$$< 1 \times \boldsymbol{label} >< 3000 \times \boldsymbol{pixel} >$$
$$< 1 \times \boldsymbol{label} >< 3000 \times \boldsymbol{pixel} > \quad (6)$$

Next step was to convert the binary file to leveldb format, because caffe only support leveldb or lmdb. We used the program provided by caffe to do the transformation. After the transformations CNN model was trained using the extracted information. After training the model it was used for the segmentation of the choroid layer. After training the model, features were extracted from the trained model. The features were mainly extracted from the pooling layer of the trained model. The reason to extract the features from this layer was that it contains the most optimized form of data with reduces number of parameters and the features were not extracted from the convolutional layers because of the sparse nature of features at these layers. The features were harvested at the output of the pooling layer. The extracted pooling layer produced feature vector of size 1024. We used these features and labels to train our SVM classifier for the segmentation of the choroid layer.

After sampling patches from all the images the sampled patches were used to train the model. The method used to train the CNN model was multinomial logistic regression (MLR). Nonlinearity was applied to the networks' output by the MLR structure. MLR was also used to apply cross entropy among the encoding of labels and normalized predictions being made by the network. The concept of weight decay was applied for the regularization of the learned variables. The sum of weigh decay and cross entropy was calculated to formulate the objective function of the network.

2.2.2 Handcrafted Features:

The handcrafted features used in our research include gabor features, gray level co-occurrence matrix and haar features.

Gabor Features:

The first handcrafted feature extracted in our research is gabor features. Gabor is basically a linear filter which is used to extract features including edges, lines and sparse features from the image. Texture representation of features can be achieved using the gabor filter as their frequency and orientation representation is very close to human visual system. Gabor features were extracted by using different orientations and frequencies on the gabor filters. Frequency in this case corresponds to the scale factor the extracted features. The frequency or scale information was extracted from exponential spacing whereas orientation information was calculated using the linear spacing approach. Scales of the gabor bank was extracted. The vector size generated using gabor features was 3072.

Haar like Features:

Edges and lines feature statistics were mainly used to extract haar features from the image dataset. This was used to train the SVM for the classification of the region of interest. The haar features explained in [27] were used to extract required information from each image to generate a feature vector. The generated features vector was then used to train the SVM.

Gray-level Co-occurrence Matrix (GLCM):

Image sub regions can analyzed with the help of GLCM as it represents the spatial and angular relation of different sub regions of the image. Co-occurrence values basically represent how often a gray level occurs horizontally, vertically or diagonally within the image. The image using GLCM is analyzed in four directions i.e. horizontally at 0 degree, vertically at 90 degree, bottom left to top right at -45 degree and top left to bottom right at

-135 degree. The vector size being extracted from the image was 8.

After extracting all the types of features, a separate support vector machine was trained using each feature.

2.3 Thickness Map of choroid layer:

next step was to calculate the thickness map for each person. So here in this step choroid layer was segmented from all 25 images corresponding to each person and then thickness was calculated at each layer in order to generate a thickness map. The thickness of each image was taken into account in order to generate the thickness map of each individual. As a result of processing each image we get a matrix representing thickness of every layer. Finally in order to get the map, matrix was resized to actual image size in order to draw the map. Fig 6 depicts the way how the thickness of choroid layer is calculated.

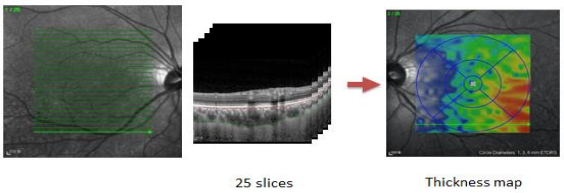

Fig 6 Choroid layer slices to calculate Thickness Map

Steps to get the thickness map:

1. For each figure, the width is 760 pixels and the height is 456 pixels.
2. Next scaling operation was applied. We can get 200 um maps 25 pixels in width, and 76 pixels in height, so we can get the true thickness of each point.
3. There are 25 figures for each patient, the interval between two figures is 240 um.
4. According to 1-3, we can map 25x760 matrix (refer to the pixel value on the figure) to 5760um x 6080um (refer to the real value of patient). And the thickness value will be mapped in different colors in the generated map. .

2.4 Support Vector Machine (SVM):

Support vector machine is a supervised algorithm which requires pre-training of data i.e. prior knowledge to carry out the classification task.

2.4.1 Classification using SVM:

Feature vectors being generated from all types of features result in quite a large number of feature vectors. As a result all the features are not used with a single classifier instead each type of feature were trained on a separate support vector machine. Let we have a training set $\{(\mathbf{x_i}, y_i)\}$, if all the data in the training set are at a distance greater than 1 form the hyper plane, then following constraints can be observed on the dataset:

$$w^T x_i + b \geq 1 \quad \text{if } y_i = 1 \qquad (7)$$

$$w^T x_i + b \leq -1 \quad \text{if } y_i = -1 \qquad (8)$$

where w is called the weigh vector and b corresponds to bias. The distance between any x_s and the hyperplane is calculated by the rescaling w and b by $\rho/2$[26]. The distance was calculated using the following expression:

$$r = \frac{y_s(\mathbf{w}^T \mathbf{x}_s + b)}{\|\mathbf{w}\|} = \frac{1}{\|\mathbf{w}\|} \qquad (9)$$

After rescaling the value of w and b, margin was calculated using the subsequent equation:

$$\rho = 2r = \frac{2}{\|\mathbf{w}\|} \qquad (10)$$

For the optimization purpose Find w and b such that

$\Phi(\mathbf{w}) = \frac{1}{2}\mathbf{w}^T\mathbf{w}$ is minimized and for all $\{(\mathbf{x_i}, y_i)\}$

$y_i(\mathbf{w}^T\mathbf{x_i} + b) \geq 1 \qquad (11)$

Finally the classification function has the following form

$$f(x) = \Sigma \alpha y x^T x + b \qquad (12)$$

The classification step basically works by formulating the inner product of the support vectors x_i and the test point x. Together with this, optimization was carried out by the inner products of $x_i^T x_j$ among all the data points used for training purpose.

After training each SVM with a different set of features vector, all the trained SVM's are linearly combined to predict a label. The purpose was to separately analyze the segmentation accuracy acquired by each type of feature. We report margin0 and margin1 precisions for feature group f, where $f \in \{GF, GLCM, Haar, Pooling\}$. For the SVM trained on f, the margin0 accuracy is the percentage of test samples for which the SVM predicted label (lf) and the true label (l) are equal. Margin1 accuracy is the percentage of test samples for which $lf \in \{l-1, l, l+1\}$.

A score value was produced for each image by considering the scores from all the classifiers which were combined linearly. The purpose of carrying this step was to gain enriched whole performance by merging the outputs of all the classifiers.

The resulting score is:

$$L_{n=(a_1 \times l_n^{GF} + a_2 \times l_n^{GLCM} + a_3 \times l_n^{Haar} + a_4 \times l_n^{Pooling}} \qquad (13)$$

Where l_n^f is the discrete label allocated to test model n by the SVM trained on feature group f.

3. Experimental Results and Discussion:

3.1 Data Set

In order to test the result of the proposed algorithm, data of real patients was collected from the Hospital Number 6 of Shanghai. The provided data from the hospital contained data of 21 individuals where each individual has 25 images, representing 25 different slices of his/her choroid layer. So the results were computed on a total of 525 images. Images of 12 individuals i.e. 300 images were used to train the model. Images of 9 persons i.e. 225 images were used to test the model.

3.2 Evaluation Matrices

In order to test the accuracy and error rate of the proposed method, two quantitative or evaluation metrics were

proposed. The purpose of introducing these metrics was to compute the error rate of the proposed method.

One metric was proposed in order to calculate the average error rate in terms of pixel values i.e. the average difference between the doctor's segmented image and the result of our proposed method. The metric can be defined as:

$$err_1 = \frac{\left\| \vec{A} - \vec{B} \right\|}{h \, x \, w}$$

Where $$\left\| \vec{A} \right\| = \sqrt{A_1^2 + A_2^2 + \cdots + A_n^2} \quad (14)$$

$\vec{A}$ is the thickness vector we computed while $\vec{B}$ is the thickness vector the doctor provided, h represents the height of the image and w is the width of the image.

Another metric was proposed to calculate the average error between the thickness map generated by doctor and the thickness map being generated by the proposed methodology. The metric can be defined as:

$$err_2 = \frac{|\bar{A} - \bar{B}|}{h}$$

Where $$\bar{A} = \frac{A_1 + A_2 + \cdots + A_w}{w} \quad (15)$$

3.3 Evaluation of the method

In order to test the results we randomly selected 25 images from the dataset and computed error rate using the above defined metrics. In order to check the accuracy of each of the feature type, 25 randomly selected images were tested using the each of the feature type. The reason was to calculate the error rate of each of the feature type. Table I represents the average mean, variance and standard deviation calculated from each of the feature type. According to the analysis of the table it can be seen that the CNN feature vector gives the minimal error rate and thus provides highest accuracy. Among the handcrafted features GLCM provided least accuracy as it can be seen in the visual results as well. Haar features provided with least error rate in handcrafted features. Table 1 represents the error rate of each of the image sing each feature type. After calculating the error rate of each image average mean, variance and standard deviation was also computed. The results can be analyzed in Table I.

Feature Type	CNN Feature Vector		Gabor Feature Vector		Haar Feature Vector		GLCM Feature Vector		Hybrid Feature vector	
Error #	err1	err2	err1	err2	err1	err2	err1	err2	err1	err2
Mean	3.7012	1.794	14.62	6.760	7.505	3.942	17.71	7.605	2.84	0.154
Variance	3.901	1.094	166.57	38.05	21.17	4.594	91.62	20.25	2.12	0.002 0
Standard Deviation	1.975	1.046	13.172	6.169	4.601	2.143	9.572	4.500	1.23	1.02

Table I: Average Mean, Variance and Standard deviation of each feature type

Mean error rate of each of the feature type in segmentation and thickness calculation can be analyzed in the graph given below:

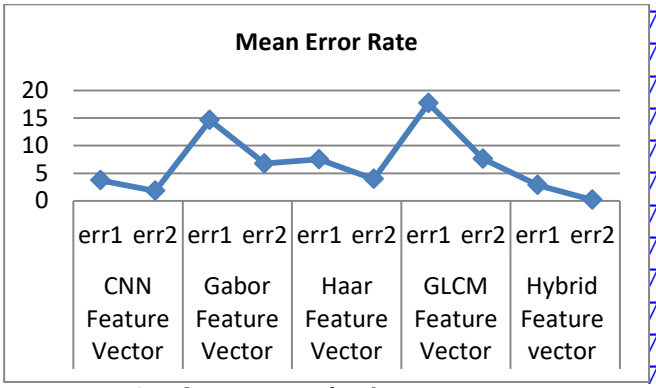

Graph1 Error rate of each Feature type

The segmentation result of each of the feature type can be analyzed in the Fig 8 given below:

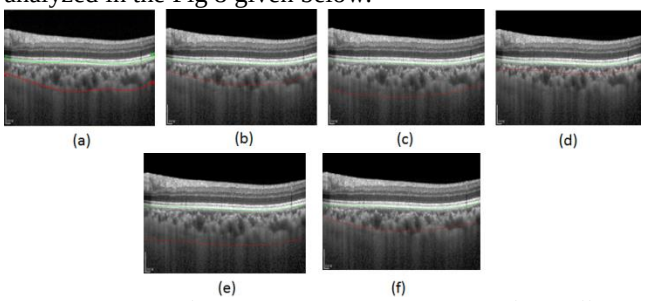

Fig 8 Comparison of choroid layer segmenation results from different feature vectorsresult, In the given figure paret (a) represents the image being labelled by the doctor, part (b) is the result of CNN feature vector, part (c) represents result of gabor feature vector, part (d)corresponds to result of GLCM, part (e) is the result of haar feature vector and lastly part (f) represents the result of hybrid approach

After calculating the error rate using each of the feature type, error rate was also computed by combining each of the features with CNN feature vector. As the CNN feature vector provided with the least error rate, it was combined linearly to find the best combination of features. The reason was to figure out an optimal accuracy with minimal feature vector and to reduce the computational time and complexity. Although the least error rate was observed when all the feature vectors were linearly combined to segment out the choroid layer.

Feature Type	CNN+ Haar feature		CNN+Gabor feature		CNN+GLCM		Hybrid Feature vector	
Error #	err1	err2	err1	err2	err1	err2	err1	err2
Mean	3.5012	1.594	7.62	3.560	12.505	6.942	2.84	0.154
Variance	2.901	0.994	102.57	18.05	67.17	13.54	2.12	0.0020
Standard Deviation	1.575	1.006	5.172	3.169	5.601	4.143	1.43	0.765

Table II: Average Mean, Variance and Standard deviation of each different combination of features

Mean error rate of each of the feature combination can be analyzed in the chart given below:

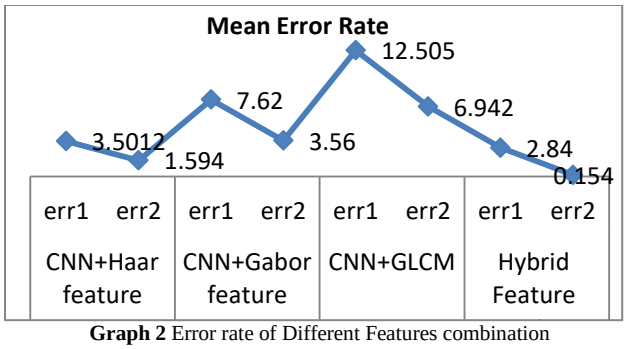

Graph 2 Error rate of Different Features combination

According to the analysis of the results it can be seen that the Haar features provided with the least error rate when combined with the CNN feature vector whereas GLCM resulted in most error rate. The table also represents the result of hybrid approach. Combination of all the features provided the most accuracy as it contains majority of the image information gathered from different types of features vector. Even if the GLCM feature vector is eliminated from the handcrafted features, it does not have much effect on the accuracy of the proposed method whereas eliminating haar features from the handcrafted features, decreased the accuracy by 4%. The CNN feature vector when combined with gabor features also provided acceptable accuracy.

The visual result of thckness map being generated by our method and doctors segmented image can be analyzed in Fig 9:

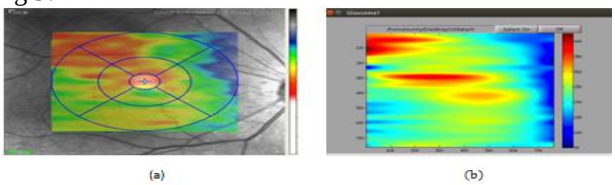

Fig 9 Thickness Map Comparison, Part (a) represents the thickness map generated by doctors segmented image where as part (b) corresponds to the thickness map generated by the proposed method

The results were than compared with few of the existing methods for choroid segmentation. The comparison of proposed method with few state of art methods can be analyzed in Table III.

Method	Mean Error Rate (Choroid Segmentation)	Mean Error Rate (Choroidal Thickness)
Automatic segmentation of choroidal thickness in optical coherence tomography [28]	3.99	4.17
Segmentation of Choroidal Boundary in Enhanced Depth Imaging OCTs Using a Multiresolution Texture Based Modeling in Graph Cuts [29]	5.99 4.30 (Grap cut Algorithm) 7.73(K-Means Algorithm)	-
Automated choroidal segmentation of 1060 nm OCT in healthy and pathologic eyes using a statistical model	14.8	-
Proposed Method	**2.84**	**0.154**

Table III: Comparison of Proposed method with some state of art methods

The results were also tested on the entire data set which provided an error rate of about 4.023 resulting in 96% accuracy. According to the visual and quantitative analysis of results it can be observed that the best results are achieved when all the feature vectors were combined together. The purpose of extracting different types of features from the image was to get accuracy in the segmentation process. As different types of features provided different type of details from the images, so combination of all the gathered information helped to accurately segment out the region of interest. The highest error rate was observed in the case of gray level co-occurrence matrix. By analyzing TABLE II it can be concluded that CNN has lower average error rate than handcrafted features and can provide more stable results as compared to handcrafted features. Using the proposed method an accuracy of up to 96 % was observed. So our model can be used to help doctors to draw the two lines automatically and compute the thickness.

4. Conclusion and Future Work

In this project, we proposed and implemented a hybrid method to automatically segment out the choroid layer. The thickness of the segmented layer was also computed. The main concern regarding measuring thickness was to analyze the choroid layer to diagnose presence of certain retinal based diseases. The results were tested using data of real patients. The results showed an accuracy of about 97%. And segmentation results were observed very similar to the segmentation carried out by the doctors. In addition we proposed two quantitative metrics for calculating the error rate of our approach. According to the computed results CNN feature vector performed better as compared to the hand crafted features. Combining all the features to segment out the choroid layer further decreased the error rate. In order to further increase the accuracy of the proposed algorithm few future directions are also mentioned below:

- Current method deals with 2D images, approach can be further extended to deal with 3D images.
- Parameters being utilized in the research can be optimized further by considering different patch sizes and optimizing stride between the extracted patches.
- The research can be extended to examine retinal based diseases like glaucoma, hypertensive retinopathy, age-related macular degeneration and macular edema.

References:

[1] Ho, Mary, et al. "Choroidal thickness measurement in myopic eyes by enhanced depth optical coherence tomography." *Ophthalmology* 120.9 (2013): 1909-1914.

[2] Adhi, Mehreen, et al. "Characterization of choroidal layers in normal aging eyes using enface swept-source optical coherence tomography." *PloS one*10.7 (2015): e0133080.

[3] Jia, Yali, et al. "Quantitative optical coherence tomography angiography of choroidal neovascularization in age-related macular degeneration."*Ophthalmology* 121.7 (2014): 1435-1444.
[4] Branchini, Lauren A., et al. "Analysis of choroidal morphologic features and vasculature in healthy eyes using spectral-domain optical coherence tomography." *Ophthalmology* 120.9 (2013): 1901-1908.
[5] D. Cabrera Fernández, H. M. Salinas, and C. A. Puliafito, "Automated detection of retinal layer structures on optical coherence tomography images," Opt. Express 13(25), 10200–10216 (2005).
[6] A. Yazdanpanah, G. Hamarneh, B. R. Smith, and M. V. Sarunic, "Segmentation of intra-retinal layers from optical coherence tomography images using an active contour approach," IEEE Trans. Med. Imaging 30(2), 484–496 (2011).
[7] A. Mishra, A. Wong, K. Bizheva, and D. A. Clausi, "Intra-retinal layer segmentation in optical coherence tomography images," Opt. Express 17(26), 23719–23728 (2009).
[8] A. Lang, A. Carass, M. Hauser, E. S. Sotirchos, P. A. Calabresi, H. S. Ying, and J. L. Prince, "Retinal layer segmentation of macular OCT images using boundary classification," Biomed. Opt. Express 4(7), 1133–1152 (2013).
[9] D. Koozekanani, K. Boyer, and C. Roberts, "Retinal thickness measurements from optical coherence tomography using a Markov boundary model," IEEE Trans. Med. Imaging 20(9), 900–916 (2001).
[10] K. A. Vermeer, J. van der Schoot, H. G. Lemij, and J. F. de Boer, "Automated segmentation by pixel classification of retinal layers in ophthalmic OCT images," Biomed. Opt. Express 2(6), 1743–1756 (2011).
[11] V. Kajić, B. Považay, B. Hermann, B. Hofer, D. Marshall, P. L. Rosin, and W. Drexler, "Robust segmentation of intraretinal layers in the normal human fovea using a novel statistical model based on texture and shape analysis," Opt. Express 18(14), 14730–14744 (2010).
[12] S. J. Chiu, X. T. Li, P. Nicholas, C. A. Toth, J. A. Izatt, and S. Farsiu, "Automatic segmentation of seven retinal layers in SDOCT images congruent with expert manual segmentation," Opt. Express 18(18), 19413–19428 (2010).
[13] E. W. Dijkstra, "A note on two problems in connexion with graphs," Numerische Mathematik 1(1), 269–271 (1959).
[14] F. LaRocca, S. J. Chiu, R. P. McNabb, A. N. Kuo, J. A. Izatt, and S. Farsiu, "Robust automatic segmentation of corneal layer boundaries in SDOCT images using graph theory and dynamic programming," Biomed. Opt. Express 2(6), 1524–1538 (2011).
[15] Q. Yang, C. A. Reisman, Z. Wang, Y. Fukuma, M. Hangai, N. Yoshimura, A. Tomidokoro, M. Araie, A. S. Raza, D. C. Hood, and K. Chan, "Automated layer segmentation of macular OCT images using dual-scale gradient information," Opt. Express 18(20), 21293–21307 (2010).
[16] B. J. Antony, M. D. Abràmoff, M. Sonka, Y. H. Kwon, and M. K. Garvin, "Incorporation of texture-based features in optimal graph-theoretic approach with application to the 3D segmentation of intraretinal surfaces in SD-OCT volumes," in SPIE Medical Imaging, (International Society for Optics and Photonics, 2012), 83141G– 83141G–83111.
[17] M. K. Garvin, M. D. Abràmoff, X. Wu, S. R. Russell, T. L. Burns, and M. Sonka, "Automated 3-D intraretinal layer segmentation of macular spectral-domain optical coherence tomography images," IEEE Trans. Med. Imaging 28(9), 1436–1447 (2009).
[18] P. A. Dufour, L. Ceklic, H. Abdillahi, S. Schröder, S. De Dzanet, U. Wolf-Schnurrbusch, and J. Kowal, "Graphbased multi-surface segmentation of OCT data using trained hard and soft constraints," IEEE Trans. Med. Imaging 32(3), 531–543 (2013).
[19] M. Haeker, M. Sonka, R. Kardon, V. A. Shah, X. Wu, and M. D. Abràmoff, "Automated segmentation of intraretinal layers from macular optical coherence tomography images," in Medical Imaging, (International Society for Optics and Photonics, 2007), 651214–651214–651211.
[20] V. Kajić, M. Esmaeelpour, B. Považay, D. Marshall, P. L. Rosin, and W. Drexler, "Automated choroidal segmentation of 1060 nm OCT in healthy and pathologic eyes using a statistical model," Biomed. Opt. Express 3(1), 86–103 (2012).
[21] L. Zhang, K. Lee, M. Niemeijer, R. F. Mullins, M. Sonka, and M. D. Abràmoff, "Automated segmentation of the choroid from clinical SD-OCT," Invest. Ophthalmol. Vis. Sci. 53(12), 7510–7519 (2012).
[22] Z. Hu, X. Wu, Y. Ouyang, Y. Ouyang, and S. R. Sadda, "Semiautomated segmentation of the choroid in spectral-domain optical coherence tomography volume scans," Invest. Ophthalmol. Vis. Sci. 54(3), 1722–1729 (2013).
[23] J. Tian, P. Marziliano, M. Baskaran, T. A. Tun, and T. Aung, "Automatic segmentation of the choroid in enhanced depth imaging optical coherence tomography images," Biomed. Opt. Express 4(3), 397–411 (2013)
[24] S. Lee, N. Fallah, F. Forooghian, A. Ko, K. Pakzad-Vaezi, A. B. Merkur, A. W. Kirker, D. A. Albiani, M. Young, M. V. Sarunic, and M. F. Beg, "Comparative analysis of repeatability of manual and automated choroidal thickness measurements in nonneovascular age-related macular degeneration," Invest. Ophthalmol. Vis. Sci. 54(4), 2864–2871 (2013).
[25] K. Li, X. Wu, D. Z. Chen, and M. Sonka, "Optimal surface segmentation in volumetric images--a graphtheoretic approach," IEEE Trans. Pattern Anal. Mach. Intell. 28(1), 119–134 (2006).
[26] Maji, Subhransu, Alexander C. Berg, and Jitendra Malik. "Classification using intersection kernel support vector machines is efficient." *Computer Vision and Pattern Recognition, 2008. CVPR 2008. IEEE Conference on*. IEEE, 2008.
[27] R Lienhart and J Maydt, "An extended set of haar-like features for rapid object detection," in *IEEE Image Processing*, 2002, pp. I900 – I903.
[28] Alonso-Caneiro, David, Scott A. Read, and Michael J. Collins. "Automatic segmentation of choroidal thickness in optical coherence tomography."*Biomedical optics express* 4.12 (2013): 2795-2812.
[29] Danesh, Hajar, et al. "Segmentation of choroidal boundary in enhanced depth imaging OCTs using a multiresolution texture based modeling in graph cuts."*Computational and mathematical methods in medicine* 2014 (2014).
[30] Kajić, V., Esmaeelpour, M., Považay, B., Marshall, D., Rosin, P. L., & Drexler, W. (2012). Automated choroidal segmentation of 1060 nm OCT in healthy and pathologic eyes using a statistical model. *Biomedical optics express*, *3*(1), 86-103.